

G β γ Recruits Rho1 to the Site of Polarized Growth during Mating in Budding Yeast*

Received for publication, December 11, 2002, and in revised form, March 20, 2003
Published, JBC Papers in Press, March 26, 2003, DOI 10.1074/jbc.M212636200

Eli E. Bar, Alexis T. Ellicott, and David E. Stone‡

From the Department of Biological Sciences, Laboratory for Molecular Biology, University of Illinois at Chicago, Chicago, Illinois 60607

In mating mixtures of *Saccharomyces cerevisiae*, cells polarize their growth toward their conjugation partners along a pheromone gradient. This chemotropic phenomenon is mediated by structural proteins such as Far1 and Bem1 and by signaling proteins such as Cdc24, Cdc42, and G β γ . The G β γ subunit is thought to provide a positional cue that recruits the polarity establishment proteins, and thereby induces polarization of the actin cytoskeleton. We identified *RHO1* in a screen for allele-specific high-copy suppressors of G β γ overexpression, suggesting that Rho1 binds G β γ *in vivo*. Inactivation of Rho1 GTPase activity augmented the rescue phenotype, suggesting that it is the activated form of Rho1 that binds G β γ . We also found, in a pull-down assay, that Rho1 associates with GST-Ste4 and that Rho1 is localized to the neck and tip of mating projections. Moreover, a mutation in *STE4* that disrupts G β γ -Rho1 interaction reduces the projection tip localization of Rho1 and compromises the integrity of pheromone-treated cells deficient in Rho1 activity. In addition to its roles as a positive regulator of 1,3- β -glucan synthase and of the cell integrity MAP kinase cascade, it was recently shown that Rho1 is necessary for the formation of mating projections. Together, these results suggest that G β γ recruits Rho1 to the site of polarized growth during mating.

Signal-induced polarized growth is a fundamental mechanism of cellular differentiation and environmental response. The function of many mammalian cell types depends on their ability to sense relevant stimuli and grow in a directed fashion. An excellent model system with which to study such chemotropic phenomena is the mating response of the budding yeast, *Saccharomyces cerevisiae*. In preparation to mate, haploid yeast of opposite mating types exchange peptide mating pheromones. The binding of pheromone to G protein-coupled receptors triggers a developmental program that ultimately blocks cell cycle progression, alters gene expression, and induces the formation of elongated projections called shmoos. These mating projections grow toward the highest concentration of pheromone and are crucial for the establishment of cell fusion (1, 2). It has recently become clear that the receptor and the G protein are the sensors of the pheromone gradient (3, 4). Chemotropic growth depends on the association between free G β γ and the

guanine nucleotide exchange factor Cdc24 through the intermediary scaffold Far1 (5, 6). Cdc24 activates the monomeric G protein, Cdc42 (6, 7), which polarizes the actin cytoskeleton and thus the growth of the plasma membrane (8). In *S. cerevisiae*, the plasma membrane is supported by a rigid cell wall composed of polysaccharides and mannoproteins (9). Presumably, growth of the plasma membrane requires growth of the cell wall. The biosynthesis of cell wall components is tightly coordinated with the construction of new cell wall (9). This coordination is partially dependent on Rho1, a monomeric G protein belonging to the same GTPase subfamily as Cdc42. Rho1 plays a dual role in cell wall biosynthesis. First, Rho1 is a regulatory subunit of the glucan synthase enzymatic complex (10). It regulates the synthesis of 1,3- β -glucan, the major component of the yeast cell wall. Second, Rho1 binds and activates the protein kinase C of yeast, Pkc1. Rho1-dependent Pkc1 activation initiates a MAP¹ kinase signaling cascade that is critical to the maintenance of cell wall integrity when the cell is stressed (11–14). Here we show that in addition to stimulating polarized growth of the plasma membrane by recruiting Cdc42, G β γ also associates with Rho1. This association is required for proper localization of Rho1 to the tip of the mating projection.

EXPERIMENTAL PROCEDURES

Molecular and Microbiological Techniques—Standard methods were used for microbial and molecular manipulation (15, 16). The *rho1^{ts}* yeast strain used in the cell lysis experiment was isolated by Saka *et al.* (43). All other yeast strains used in this study were derived from strain 15Dau (*MATa bar1 Δ ade1 his2 leu2–3,–112 trp1 ura3 Δ*), which is isogenic with strain BF264–15D (17). Both strains A35 and ELY115 contain the *STE4*^{A405V} allele at the *STE4* locus. Strain A35 is the original mutant *STE4* isolate (18). It was back-crossed three times prior to use in this study. Strain ELY115 was created by replacing *STE4* with *STE4*^{A405V} in the wild type 15Dau background (18). Yeast transformations were performed by the lithium acetate method (19). *Escherichia coli* transformations were performed by electroporation (16). The plasmids used in this study are listed in Table I. Plasmids YCplac33/GAL1-*STE4* and YCplac33/GAL1-*STE4*^{A405V} were constructed as follows: *STE4* was PCR-amplified from YCplac33/*STE4* and YCplac33/*STE4*^{A405V} (18) with added *Bam*HI-*Eco*RI ends. The priming oligonucleotides were: 5'-CGGGATCCCTGTACAGCTCAATCA-3' and 5'-CGGAATTCGTAGGGACAGCCATCATG-3' (boldface letters indicate the bases that comprise the added restriction sites). The products were subcloned into the pCRII vector (Invitrogen), and subsequently subcloned as *Bam*HI fragments into YCpLac33/GAL. PYES2.0/GAL1-RHO1 was created as follows: *RHO1* was PCR-amplified using strain 15Dau genomic DNA as template, and the product was cloned into the pYES2.0 vector (Invitrogen) as a *Bam*HI-*Eco*RI fragment. The priming oligonucleotides were: 5'-CGGGATCCCTGCACTAATAGAAAATCATAGAAC-3' and 5'-GGGAATTC AAAGGCATACGTACATACAATAGA-3'.

* This work was supported by American Cancer Society Research Grant RPG-94-034-06-MBC and by National Science Foundation Grant MCB-0111 397. The costs of publication of this article were defrayed in part by the payment of page charges. This article must therefore be hereby marked "advertisement" in accordance with 18 U.S.C. Section 1734 solely to indicate this fact.

‡ To whom correspondence should be addressed. Tel.: 312-996-5710; Fax: 312-413-2691; E-mail: dstone@uic.edu.

¹ The abbreviations used are: MAP, mitogen-activated protein; MEK, mitogen-activated protein kinase/extracellular signal-regulated kinase; GST, glutathione S-transferase; TBS, Tris-buffered saline; HA, hemagglutinin; GFP, green fluorescent protein; RID, Rho1 interaction domain.

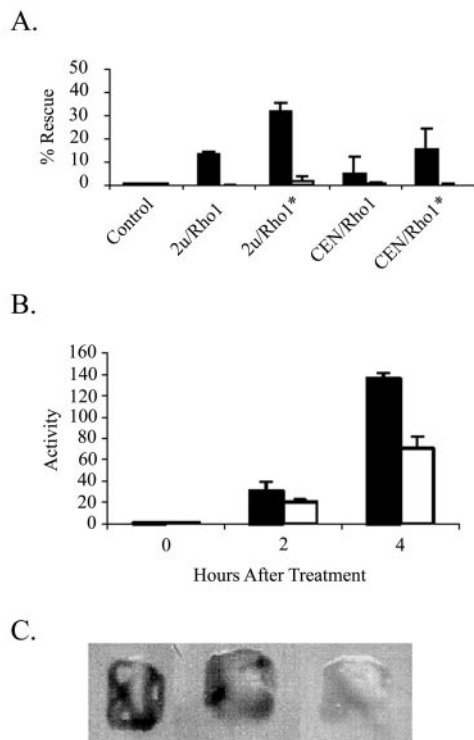


FIG. 1. The effect of Rho1 activation and overexpression on mating pathway signaling. *A*, colony formation assays. Strain 15Dau was cotransformed with either the *GAL1-STE4* (closed bars) or *GAL1-STE4*^{A405V} (open bar) plasmids, along with low-copy (*CEN*) or high-copy (2 μ) *RHO1* plasmids. Rho1* indicates the activated (Q68H) form of *RHO1*. Transformants were grown to saturation in galactose medium, and the relative ability of each strain to form colonies was determined as described under "Experimental Procedures." *B*, pheromone-induced transcription assay. Strain 15Dau was cotransformed with either the pYES2.0/Gal1-Rho1 or pYES2.0 plasmids along with the *FUS1-lacZ* reporter plasmid, pSB231. Transformants were grown to mid-log phase in galactose medium and treated with 15 nM α -factor. Aliquots were taken at the indicated time points, and β -galactosidase activity was determined as described under "Experimental Procedures." The closed bars correspond to the pYES2.0 cells and the open bars to the pYES2.0/Gal1-Rho1 cells. *C*, epistasis analysis. 15Dau cells transformed with pSB231 and the following plasmids were grown to saturation on solid medium containing galactose: left, *GAL1-STE4*; middle, *STE11-4* and *GAL1-RHO1*; right, *GAL1-STE4* and *GAL1-RHO1*. β -Galactosidase activity was then assayed as described under "Experimental Procedures."

pEB15.0 was created as follows: *RHO1* was PCR-amplified from strain 15Dau genomic DNA, and the product was cloned into pESC-URA (Stratagene, La Jolla, CA) as a *KpnI-XhoI* fragment, thereby placing *RHO1* under *GAL1* promoter control. The priming oligonucleotides were: 5'-CCGCTCGAGATGTCAACAAG TTGGTAAC-3' and 5'-CGGGGTACCCTATAACAAGACACATTTTC-3'. *FAR1* was PCR-amplified from strain 15Dau genomic DNA, and the product was cloned into pESC-URA as a *PacI-BglII* fragment, thereby placing *FAR1* under *GAL10* promoter control. The priming oligonucleotides were: 5'-CCTTAATTAAGCGTAGTATAGACGTGGAG-3' and 5'-GAAGATCT-TGAAGACACCAACAAGAGTTTCG-3'. pEB13.0 was created as follows: *STE4* was PCR-amplified from 15Dau genomic DNA, and the product was cloned into pYEX4T-1 (Clontech Lab. Palo Alto, CA) as an *EcoRI* fragment. The priming oligonucleotides were: 5'-CGGAATTCATGGCAGCATCAGATGG-3' and 5'-GAATTCACAGTATTTTCAATTTCG-3'. The resulting CUP1-GST-STE4 hybrid gene was then excised as a *PvuII-NdeI* fragment. Its ends were blunted using Klenow fragments and subcloned into *PvuII*-digested YCplac111. pEB13.2 was created by subcloning the blunt-ended *PvuII-NdeI* CUP1-GST fragment from pYEX4T-1 to YCplac111. pEB13.1 was created by converting the wild type *STE4* allele of pEB13.0 to *STE4*^{A405V} using the QuikChangeTM mutagenesis kit (Stratagene). The mutagenic primers were: 5'-GTCCAGATGGGTAGTTGTATGTACAGGTTCA-3' and 5'-CCTGTACATACAATAACCATCTGGACTCG-3' (the mutagenic bases are indicated in boldface and underlined). pEB13.5 was created as follows: PKC1³⁷⁸⁻⁶⁴⁰ (PKC1^{RID}) was PCR-amplified from pGAD424/

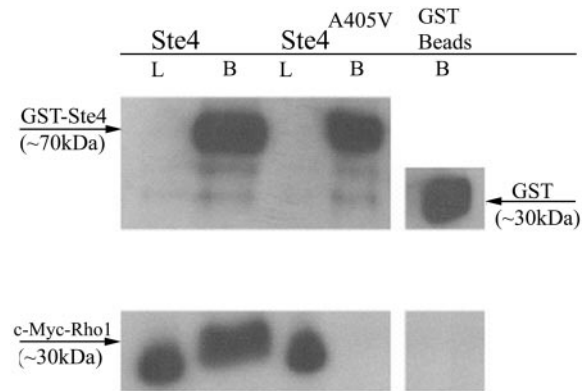


FIG. 2. Association of Rho1 with Ste4. Lysates of 15Dau overexpressing cMyc-Rho1, His₆-Ste18, and either GST-Ste4 (first and second lanes from left), GST-Ste4^{A405V} (third and fourth lanes), or GST (fifth lane) were incubated with glutathione beads. The bound proteins were resolved on SDS-PAGE and immunoblotted with anti-GST (upper panel), and anti-cMyc (lower panel). B, bound proteins; L, protein load.

PKC1. The priming oligonucleotides were: 5'-GCGAAGATCTACAC-TAGGATTCCACAAGTC-3' and 5'-CCGCTCGAGCGGGGCTCATTTCATCGA-3'. The PCR product was digested with *BglII* and *XhoI* and subcloned into *BamHI/XhoI*-digested pEB13.2. pEB18.0 was created as follows: PKC1^{RID} was PCR-amplified from pGAD424/PKC1. The priming oligonucleotides were: 5'-TCCCCGCGGGGAATGACACTAGGATTCCACAAGTC-3' and 5'-TCCCCGCGGGGACTCATTTTCATCGATAA-ATTATTTAG-3'. The PCR product was digested with *SacII* and ligated to *SacII*-digested pRS316CG. YCplac22/GAL1-His₆-STE18 was created as follows: *STE18* was PCR-amplified from 15Dau genomic DNA. The priming oligonucleotides were: 5'-GGATCCATGCATCACC-ATCACCATCACATGACATCAGTTCAAAACTC TCCACGC-3' and 5'-GAAGCTTTTACATAAGCGTACAACAAACAC-3'. The PCR product was ligated into PCRII (Invitrogen), and subsequently subcloned into YCplac22/GAL1 as a *BamHI-HindIII* fragment. The *GAL1-RHO1* transcriptional fusion identified in the screen was isolated from a cDNA library kindly provided by Stephen J. Elledge. Plasmids pRS315/RHO1, pRS425/RHO1, pRS315/RHO1^{Q68H}, and pRS425/RHO1^{Q68H} were kindly provided by Alan M. Myers (20).

β Y Allele-specific High-copy Suppressor Screen—Strain ELY105 (a derivative of strain 15Dau containing an integrated copy of *GAL1-STE18*) was transformed first with YCplac33/GAL1-STE4 and subsequently with the yeast pTRP1 c-DNA library (kindly provided by Stephen Elledge). Transformants were spread on selective sucrose medium lacking uracil and tryptophan. Approximately 100,000 colonies were then replica-plated to selective dextrose or to selective galactose medium lacking uracil and tryptophan. Rescue of growth arrest was verified, and sterile mutants were discarded. The YCplac33/GAL1-STE4 plasmid was cured using 5-fluoroorotic acid, and the strains were transformed with YCplac33/GAL1-STE4^{A405V}. The ability of the library clone to rescue overexpression of *STE4*^{A405V} was then determined. Library clones that showed allele specificity were characterized further.

Colony Formation Assays—Colony formation assays were performed by spreading 750 cells on the appropriate selective medium containing a range of α -factor concentrations. Plates were incubated at 30 °C for 3–5 days. Resistance to α -factor was quantified by determining the percent survival on medium containing 3, 6, 15, 30, and 60 nM α -factor as compared with the number of colonies that formed on medium lacking pheromone.

***FUS1* Expression Assays**—Expression of the pheromone-inducible *FUS1* transcript was assayed by measuring β -galactosidase levels in cells containing a *FUS1-lacZ* reporter gene. Strain 15Dau was transformed with the *FUS1-LacZ* reporter vector (pSB231) (21) and either pYES2 or pYES2/GAL1-RHO1. Cultures were grown at 30 °C to an A₆₀₀ of 0.5 in selective galactose medium. α -Factor was added to a final concentration of 15 nM, and the cultures were shaken at 30 °C. Cells were harvested, and β -galactosidase activity was determined as described previously (22). To assay β -galactosidase in cells grown on solid medium, nitrocellulose lift assays were performed as described (23).

Immunoblots—Yeast whole cell extracts were prepared by bead beating and clarified by centrifugation. 15 μ g of total protein/well was electrophoresed on discontinuous SDS-polyacrylamide gels and electroblotted to polyvinylidene difluoride membranes (PVDF-PLUS, MSI Inc., Westborough, MA) according to the manufacturer's protocol. Blots

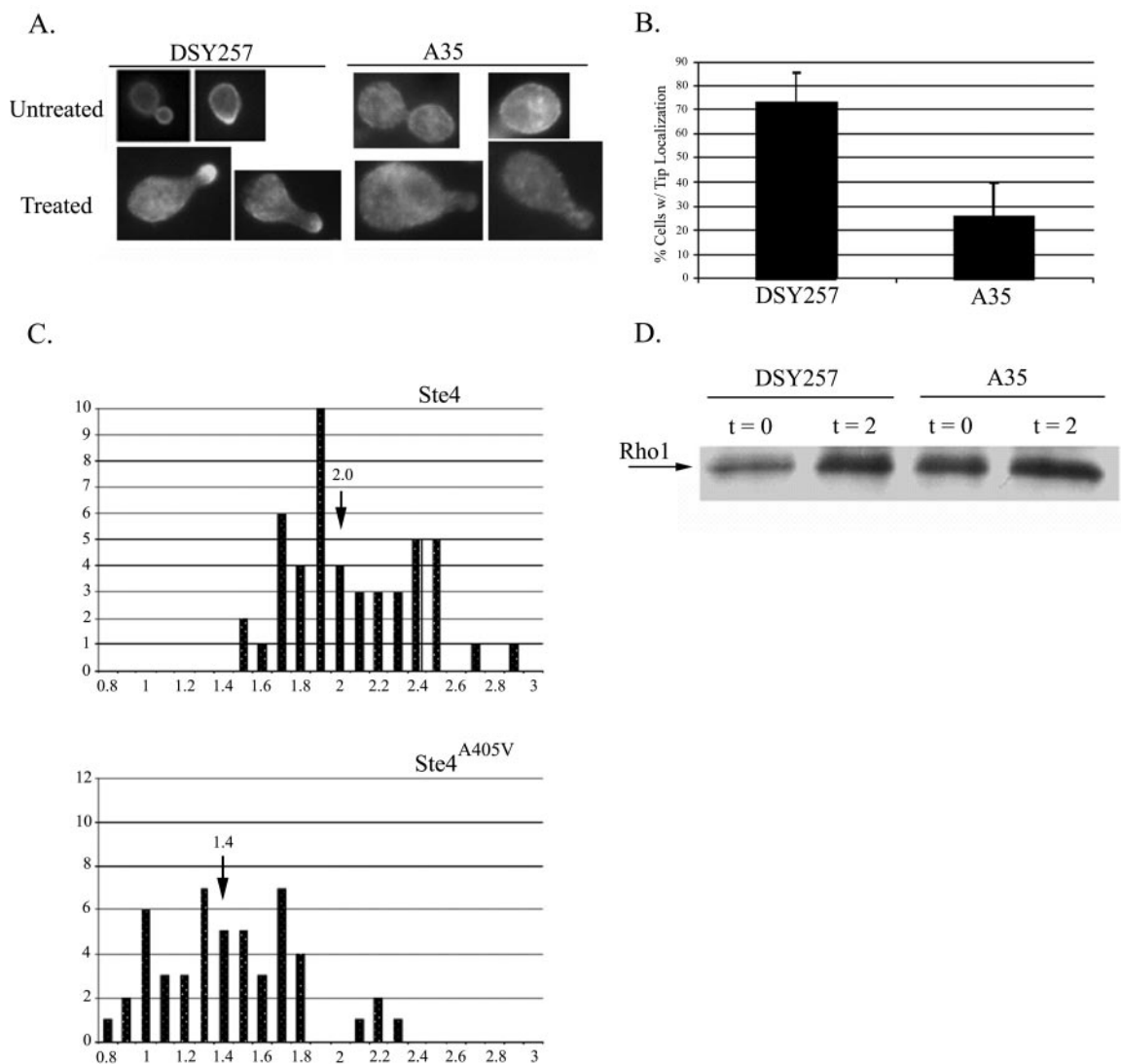


FIG. 3. Localization of Rho1 before and after pheromone treatment. 15Dau cells transformed with pHA-RHO1 were grown to mid-log phase, and the localization of HA-Rho1 was determined by immunofluorescence before and 2 h after treatment with 30 nM α -factor. Aliquots were also taken to determine the relative levels of HA-Rho1 in each culture. **A**, representative photomicrographs of wild type (strain DSY257) and *STE4^{A405V}* (strain A35) cells. **B**, bar graphs indicating the percent wild type (strain DSY257) and *STE4^{A405V}* (strain A35) cells that showed a detectable concentration of HA-Rho1 at the shmoo tip. The mean values and standard deviations were calculated from three independent experiments. **C**, quantitation of the relative HA-Rho1 concentration at shmoo tips. The relative tip fluorescence for populations of wild type and *STE4^{A405V}* cells was determined as described under "Experimental Procedures," and the distribution of values represented in histograms. The number of cells (y axis) is plotted as a function of the relative tip fluorescence values (x axis). The distributions of values represented in histograms. The arrows on the histograms indicate the mean value for each of the sampled populations. **D**, Western blot showing the relative levels of HA-Rho1 in the wild type (strain DSY257) and *STE4^{A405V}* mutant (strain A35) cells used in the localization experiments. Aliquots were taken for analysis before ($t = 0$) and 2 h after ($t = 2$) treatment with pheromone.

were then blocked with 5% nonfat dry-milk in TBS (20 mM Tris-HCl, pH 7.5, 500 mM NaCl) for 1 h and incubated with a 1:2000 dilution of a rabbit anti-GST antibody (Santa Cruz Biotechnology, Inc., Santa Cruz, CA) or a 1:500 dilution of the 9E10 mouse anti c-Myc antibody (Santa Cruz). Membranes were incubated at 4 °C overnight and then washed three times with TBS plus 0.2% Tween for 10 min. The washed membranes were probed with either horseradish peroxidase-conjugated goat anti-rabbit antibody (Promega, Madison, WI) or horseradish peroxidase-conjugated sheep anti-mouse antibody (Amersham Biosciences). Membranes were washed three times with TBS plus 2% Tween, and peroxidase activity was visualized using ECL (Amersham Biosciences) and Fuji RX film (Fuji Medical Systems, Stamford, CT).

GST Pull-down—Yeast strains EBY185, EBY186, and EBY187 were derived from strain 15Dau by transformation. They each carry the YCplac22/GAL1-His₆-STE18 and pEB15.0 plasmids. In addition, EBY185 carries the pEB13.0 plasmid, EBY186 carries the pEB13.1 plasmid, and EBY187 carries the pEB13.2 plasmid. All three strains were grown in selective medium at 30 °C to an A_{600} of 0.4, at which point galactose was added to a final concentration of 3%. Cultures were

then split and incubated for 2 h at 30 °C. α -Factor was added to a final concentration of 15 nM, and the cultures were incubated for an additional 4 h. Cells were visualized by phase-contrast light microscopy to confirm mating projection formation in the treated cultures. Cells were harvested by centrifugation, washed once with cold water, and frozen in liquid nitrogen. Upon thawing, cell pellets were washed once with TBS and lysed with glass beads in radioimmune precipitation buffer (50 mM Tris, pH 7.5, 1% sodium deoxycholate, 1% Triton X-100, 1 mM NaPP_i, 150 mM NaCl, 1 mM Na₃VO₄, 50 mM NaF). Protease inhibitors were added just before lysis: 1 mM phenylmethylsulfonyl fluoride (Roche Applied Science), 1 μ g/ml pepstatin A, 1 μ g/ml leupeptin, and 5 μ g/ml aprotinin (Sigma). The crude lysates were cleared by centrifugation at 12,000 rpm for 15 min. Protein concentration was determined using the Bio-Rad protein assay kit. For each sample, 1 mg of total protein was transferred to a chilled microcentrifuge tube containing 20 μ l of glutathione-Sepharose 4B (Amersham Biosciences); the tubes were incubated for 30 min at room temperature and then for an additional 30 min at 4 °C. The beads were washed several times with phosphate-buffered saline supplemented with the protease inhibitor mixture described

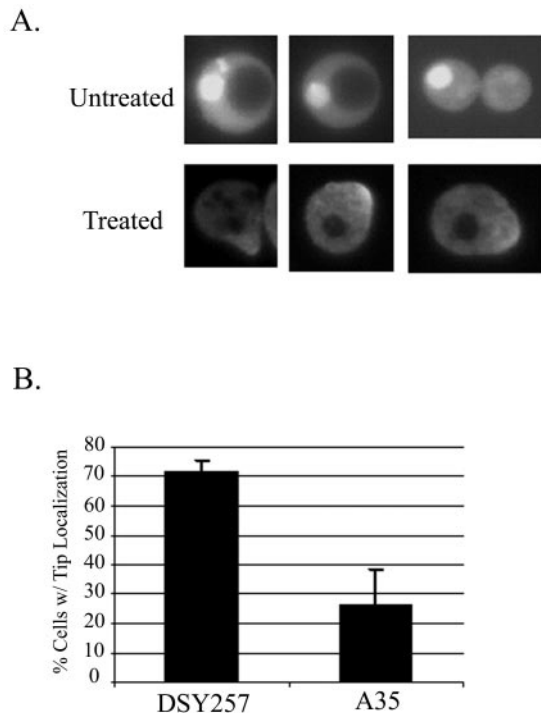


FIG. 4. **Localization of Pkc1^{RID}-GFP.** 15Dau cells transformed with pEB18.0 (PKC1^{RID}-GFP) were grown to mid-log phase, and the localization of Pkc1^{RID}-GFP was determined by fluorescent microscopy before and 2 h after treatment with 30 nM α -factor. **A**, representative photomicrographs of wild type (strain DSY257) cells. **B**, bar graphs indicating the percent wild type (strain DSY257) and *STE4*^{A405V} (strain A35) cells that showed a detectable concentration of Pkc1^{RID}-GFP at the shmoo tip. The mean values and standard deviations were calculated from three independent experiments.

above. To elute the bound proteins, 50 μ l of sample loading buffer was added, and the samples were boiled for 3 min. Samples were subjected to SDS electrophoresis.

Immunofluorescence—Strains 15Dau, A35, and ELY115 were transformed with pHA-RHO1 and grown to mid-log phase in selective medium at 30 °C. The localization of HA-Rho1 was determined by immunofluorescence before and 2 h after treatment with 30 nM α -factor. Cells were prepared for immunofluorescent microscopy as described previously (15). The primary antibody, 12CA5 (Roche Diagnostics), was incubated with the immobilized cells at a dilution of 1:500, and the fluorescein isothiocyanate-conjugated anti-mouse secondary antibody (Santa Cruz) was diluted 1:2000. Fluorescent images were acquired using a Zeiss Axioskop 2 microscope fitted with a Zeiss AxioCam digital camera and processed using Zeiss AxioVision software.

PKC1^{RID}-GFP Visualization—Strains 15Dau, A35, and ELY115 were transformed with pEB18.0 and grown to mid-log phase in selective medium at 30 °C. The expression of PKC1^{RID}-GFP was induced by adding CuSO₄ to a concentration of 0.5 mM. The localization of Pkc1^{RID}-GFP was visualized before and 2 h after treatment with 30 nM α -factor. Live cells were scored for the presence of Pkc1^{RID}-GFP at the mating projection tip using a Zeiss Axioskop 2 microscope.

Photomicrographs and Quantification of HA-Rho1 Localization—Fluorescent images were acquired using a Zeiss Axioskop 2 microscope fitted with a Zeiss AxioCam digital camera and processed using Zeiss AxioVision software. Localization of HA-Rho1 was quantified from the digital images using the histogram function of Adobe Photoshop, version 5.5. A circle of set size was used to sample the brightness of the projection tip and a peripheral point directly opposite the tip of cells from randomly chosen fields. The ratio of tip to bottom fluorescence was rounded to the nearest 0.1, and values corresponding to 50 cells for each strain were plotted in histograms.

Cell Lysis Assay—Cells were grown at 23 °C in selective media to a density of A₆₀₀ = 2.5, and then 4 ml of each culture was harvested and resuspended in 1 ml of rich medium (YEPA medium, containing 1% yeast extract (Difco Laboratories), 2% Bacto-Peptone (Difco), and 2% glucose). After incubation at 23 °C for 4 h, the cells were pelleted again and resuspended in 40 μ l of YEPA. 10 μ l of each suspension was spotted onto YEPA plates and on YEPA plates supplemented with 150 nM

α -factor. After incubation at room temperature overnight, the lysis assay was performed as described previously (24). Digital images of the plates were acquired after 2 h at room temperature.

RESULTS

Rho1 Associates with Ste4—On the basis of genetic and structural evidence, we have inferred that an unknown protein binds and down-regulates the $\beta\gamma$ subunit of the pheromone responsive G protein. G β and G γ are encoded by the *STE4* and *STE18* loci, respectively. A tight cluster of mutations in *STE4* (A405V, G409D, S410L, and W411L/S) disrupts interaction with the putative regulator (18). To identify the unknown element, we took advantage of the observation that G $\beta\gamma$ overexpression strongly induces the mating signal and thereby confers permanent cell cycle arrest (25–27). Plasmids were constructed that allow for the galactose-inducible expression of G β (*GAL1-STE4*) and G γ (*GAL1-STE18*). A high-copy *GAL1*-cDNA yeast library was then screened for plasmids that could rescue the overexpression of wild type G $\beta\gamma$. Plasmids recovered in this step were re-screened for the inability to rescue the overexpression of a mutant form of G $\beta\gamma$, encoded by *STE4*^{A405V} and *STE18*. We reasoned that genes identified in this allele-specific screen might encode proteins that interact with Ste4. Of the 250,000 transformants screened, the most frequently isolated plasmid contained *RHO1*. Rho1 is a highly conserved and well studied monomeric G protein. The mammalian homologue of Rho1, RhoA, is involved in polarization of the actin cytoskeleton. It has also been implicated in transcription, adhesion, and transformation (28–30). Like mammalian Rho proteins, Rho1 is thought to play a role in polarization of the actin cytoskeleton (10, 31). However, it also stimulates 1,3- β -glucan synthase (10, 32) and the cell integrity MAP kinase cascade (33, 34), both of which are necessary for growth of the yeast cell wall.

To confirm and quantitate the effect of Rho1 overexpression on G $\beta\gamma$ -induced lethality, we performed single-colony formation assays. Strain 15Da (17) was co-transformed with either the wild type or mutant G $\beta\gamma$ -overexpressing plasmids and either *RHO1* low-copy, *RHO1* high-copy, or control plasmids. Transformants were plated on glucose and on galactose medium, respectively, to repress and induce expression of G $\beta\gamma$. Only about 0.5% of the cells overexpressing wild type G $\beta\gamma$ in the absence of excess Rho1 were able to form colonies (Fig. 1A). In contrast, about 5% of the cells transformed with the low-copy number *RHO1* plasmid and about 13% of the cells transformed with the high-copy number *RHO1* plasmid could overcome the excess G $\beta\gamma$ and form colonies. Interestingly, overexpression of a mutationally activated form of Rho1, *RHO1*^{Q68H}, enhanced the rescue phenotype by about 3-fold. However, neither Rho1 nor Rho1^{Q68H} could significantly increase the plating efficiency of cells forced to overexpress the mutant form of G $\beta\gamma$. The simplest interpretation of these data is that excess Rho1 antagonizes G $\beta\gamma$ -induced cell cycle arrest by directly interacting with Ste4. A less likely possibility is that Rho1 rescues cells overexpressing G $\beta\gamma$ by promoting cell cycle progression rather than by relieving the inhibitory effects of the mating signal. To distinguish these hypotheses, we assessed the effect of Rho1 overexpression on mating specific transcription using a *FUS1-lacZ* reporter. The reporter was stimulated either by treating cells with pheromone or by expression of Ste11-4, a dominant mutant form of the Ste11 MEK kinase that constitutively activates the mating pathway (35). Excess wild type Rho1 reduced pheromone-induction of *FUS1-lacZ* by about 50% (Fig. 1B) but had no effect on the activity of Ste11-4 (Fig. 1C). Thus, Rho1 overexpression inhibits the effects of free G $\beta\gamma$ on both transcription and cell cycle progression, and it does so at or above the level of the MEK kinase.

TABLE I
Plasmids used in this study

Plasmid	Markers/constructs	Source
YCplac33/GAL1-STE4	URA3 CEN GAL1-STE4	This study
YCplac33/GAL1-STE4 ^{A405V}	URA3 CEN GAL1-STE4	This study
YCplac33/STE4	URA3 CEN STE4	(18)
YCplac33/STE4 ^{A405V}	URA3 CEN STE4 ^{A405V}	(18)
YCplac111/GAL1-STE18	LEU2 CEN GAL1-STE18	This study
pEB15.0	URA3 2 μ GAL1-cMyc-RHO1; GAL10-FLAG-FAR1	This study
pEB13.0	LEU2 CEN CUP1-GST-STE4	This study
pEB13.1	LEU2 CEN CUP1-GST-STE4 ^{A405V}	This study
pEB13.2	LEU2 CEN CUP1-GST	This study
YCplac22/GAL1-His ₆ -STE18	TRP1 CEN GAL1 His ₆ -STE18	This study
pEB13.5 (PKC1 ^{RID})	LEU2 CEN CUP1-PKC1 ³⁷⁸⁻⁶⁴⁰	This study
pEB18.0 (PKC1 ^{RID} -GFP)	URA3 CEN CUP1-GFP-PKC1 ³⁷⁸⁻⁶⁴⁰	This study
PYES2.0/GAL1-RHO1	URA3 2 μ GAL1-RHO1	This study
pRS315/RHO1	LEU2 CEN RHO1	(8)
pRS315/RHO1 ^{Q68H}	LEU2 CEN RHO1 ^{Q68H}	(8)
pRS425/RHO1	LEU2 2 μ RHO1	(8)
pRS425/RHO1 ^{Q68H}	LEU2 2 μ RHO1 ^{Q68H}	(8)
pSB231	URA3 CEN FUS1- <i>lacZ</i>	(21)
pSL1509	URA3 CEN STE11-4	(35)
pRS316-2XHA-RHO1	URA3 CEN HA-RHO1	(39)
pGAD424/PKC1	LEU2 2 μ GAL4AD-PKC1	(40)
pRS316CG	URA3 CEN CUP1-GFP	(50)

To further evaluate the possibility that G $\beta\gamma$ physically interacts with Rho1, we constructed tagged versions of Ste4, Ste18, and Rho1, and performed pull-down assays. The tagged forms of all three proteins proved to be functional (data not shown). As shown in Fig. 2, myc-Rho1 specifically associated with GST-Ste4 but failed to associate with GST-Ste4^{A405V} or GST alone. Interestingly, the Far1 protein, which links G $\beta\gamma$ with Bem1 and Cdc42, also failed to associate with GST-Ste4^{A405V} (data not shown).

The Localization of Rho1 to the Tips of Mating Projections Depends on Ste4—In dividing cells, Rho1 associates with cortical actin patches, concentrating at the site of bud emergence, the tip of growing buds, and the mother-bud neck region prior to cytokinesis (31, 36). This subcellular localization of Rho1 is consistent with its role in stimulating cell wall biogenesis through interaction with 1,3- β -glucan synthase and Pkc1. Given that G $\beta\gamma$ concentrates at the tips of mating projections (37), and that G $\beta\gamma$ and Rho1 interact (Figs. 1 and 2), we would expect to find Rho1 at the tips of mating projections as well. Indeed, Rho1 has been reported to exhibit “polarized localization” when stationary cells are treated with pheromone (38). To confirm and extend this observation, we examined the localization of an HA-tagged form of Rho1 (39). As expected, HA-Rho1 was found at the periphery of vegetative cells and was concentrated at the tips of mating projections after pheromone treatment (Fig. 3A). We also observed HA-Rho1 in a ring at the mating projection neck (data not shown). To determine whether the shmoo tip localization of Rho1 depends on its association with Ste4, we compared the localization of HA-Rho1 in wild type and STE4^{A405V} cells (Fig. 3, A and B). Although the two strains exhibited identical HA-Rho1 staining patterns during vegetative growth, HA-Rho1 was clearly mislocalized in a large fraction of the STE4^{A405V} cells following pheromone treatment. Whereas ~72% of the responsive wild type cells showed a detectable concentration of HA-Rho1 at the shmoo tip, tip localization was apparent in only about 25% of the mutant cells. Furthermore, the fraction of mutant cells in which HA-Rho1 did localize to the projection tips exhibited significantly less polarized accumulation of the reporter than did the wild type cells. A quantitative assay showed the tips of the wild type shmoos to be, on average, twice as bright as their bottoms, whereas the average mutant shmoo was only 40% brighter at its tip than at its bottom (Fig. 3C). *t* test analysis of the data showed this difference to be highly significant (*p* <

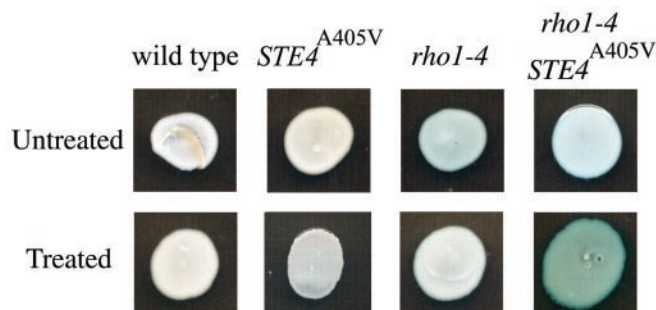


FIG. 5. Effect of *rho1-4* and STE4^{A405V} on cell integrity. Cells were grown and assayed for lysis as described under “Experimental Procedures.” Vegetative cells are shown in the upper row. Pheromone-treated cells are shown in the lower row. From left to right, the strains are as follows: 1) wild type (YOC1943); 2) ELY112, an STE4^{A405V} derivative of strain 15dau (18); 3) EBY246, a derivative of strain YOC774 (43) of relevant genotype *rho1-4 ste4* Δ YCplac33/STE4; 4) EBY247, a derivative of strain YOC774 of relevant genotype *rho1-4 ste4* Δ YCplac33/STE4^{A405V}. The results of this experiment were identical in three independent trials.

0.0001). STE4^{A405V} cells are supersensitive to pheromone (18), and thus these results cannot be attributed to poor responsiveness or, as shown in Fig. 3D, to a low level of HA-Rho1. Therefore, the reduced tip localization of HA-Rho1 in STE4^{A405V} cells indicates that G $\beta\gamma$ plays a role in recruiting Rho1 to the site of polarized growth in mating cells.

Because inactivating the GTPase function of Rho1 augments its ability to rescue G $\beta\gamma$ overexpression (Fig. 1A), we wondered whether G $\beta\gamma$ preferentially associates with the activated form of Rho1. To answer this question, we took advantage of the finding that an internal domain of Pkc1, residues 378–640, specifically binds to activated Rho1 in the two-hybrid assay (40). We fused this Rho1 interaction domain (RID) in-frame with the gene encoding green fluorescence protein (GFP). The resulting reporter, Pkc1^{RID}-GFP, was then used to probe the subcellular localization of active Rho1. An analogous reporter was used to monitor the localization of active Rac1 (41), another monomeric G protein of the Rho class. Surprisingly, Pkc1^{RID}-GFP concentrated in the nuclei of vegetative cells (Fig. 4A). When cells were stimulated with pheromone, however, Pkc1^{RID}-GFP concentrated at the tips of the mating projections (Fig. 4A), perfectly mimicking the staining pattern of HA-Rho1 under the same conditions (Fig. 3A). We next compared the

localization of Pkc1^{RID}-GFP in wild type and *STE4*^{A405V} cells responding to pheromone. As we found when assaying the localization of HA-Rho1, the localization of Pkc1^{RID}-GFP to the tips of mating projections was significantly reduced in the mutant cells (Fig. 4B). This result suggests that it is the activated form of Rho1 that associates with G β γ at the shmoo tip.

STE4^{A405V} and *rho1-4* Confer a Synthetic Defect in the Integrity of Pheromone-treated Cells—Rho1 is essential for projection formation (31), presumably because it is essential for cell wall synthesis at the shmoo tip. If recruitment of Rho1 to the growth site is necessary for this process, then how are *STE4*^{A405V} cells able to shmoo? First, it is clear that *STE4*^{A405V} cells are only partially defective in localizing Rho1 to the shmoo tip. Perhaps the mutant form of G β γ is not completely deficient in Rho1 recruitment, or perhaps Rho1 is attracted by additional factors at the growth site. Second, Sekiya-Kawasaki *et al.* (42) have recently found that only about 20% of the normal 1,3- β -glucan synthase activity is required for viability (Table 3 in Ref. 42), suggesting that the synthesis of 1,3- β -glucan is not limiting. The abundance of 1,3- β -glucan synthase activity may mask the functional significance of the G β γ -Rho1 interaction during mating projection formation. To test this possibility, we used a *rho1* temperature-sensitive strain, YOC754 (43), which manifests a 5-fold reduction in Rho1 activity at room temperature. The native copy of *STE4* was deleted in YOC774, and the *ste4* Δ derivative strain was transformed with centromeric vectors containing *STE4* and *STE4*^{A405V}. We expected the combination of *STE4*^{A405V} and low Rho1 activity to confer a defect in cell wall biosynthesis at the tips of mating projections and, ultimately, a loss of cell integrity. Loss of cell integrity can be detected easily by overlaying cell patches with a solution containing 5-bromo-4-chloro-3-indoyl phosphate, a colorimetric substrate that is cleaved to a blue product by the alkaline phosphatase released from cells upon lysis. For reasons that are not clear, the *rho1*^{ts} strain and its ancestral wild type strain (YOC1943) form mating projections very inefficiently. Only about 5% of these cells shmoo in response to 150 nM α -factor. Nevertheless, despite minimal induction of polarized growth, the combination of the *rho1*^{ts} and *STE4*^{A405V} alleles conferred a pheromone-induced increase in cell lysis (Fig. 5). Neither the *rho1*^{ts} nor the *STE4*^{A405V} single-mutant strains exhibited increased lysis upon pheromone treatment. Thus, there is a critical threshold of Rho1 recruitment to the shmoo tip below which cell integrity is compromised.

DISCUSSION

Signal-induced polarization is essential in development and in the differentiated function of many cell types. For example, neuronal growth cones respond to chemoattractants during nervous system development (44), fibroblasts move toward locally released platelet-derived growth factor during wound healing (45), and cell migration is guided by epidermal growth factor receptor signaling during *Drosophila* oogenesis (46). In vegetative yeast cells, growth is polarized toward the daughter cell by internal cues. Upon pheromone treatment, the axis of polarity is reoriented in response to the chemical gradient. Free G β γ binds to Far1, which acts as a scaffold on which Cdc24, Cdc42, and Bem1 are assembled. This complex is thought to polarize the actin cytoskeleton so that the plasma membrane grows toward the source of pheromone. In order for the cell to elongate, however, the cell wall must grow along with the plasma membrane, a process that requires Rho1.

Two previous studies have demonstrated direct interaction between RhoA, a mammalian homologue of Rho1, and G β subunits (47, 48). However, the functional importance of the G β -Rho interaction was not elucidated in either study. More recently, Thodeti *et al.* (49) discovered an agonist-induced

association between G β γ and active RhoA in solubilized membrane fractions from mammalian cells; they inferred that G β γ participates in targeting active RhoA to the plasma membrane. We have found that Rho1 interacts with Ste4 (G β) in an allele-specific manner: The activated form of Rho1 associates with the wild type but not the *STE4*^{A405V} mutant form of G β γ . By studying the effects of disrupting Ste4-Rho1 association on intact yeast cells, we have demonstrated the functional importance of a G β γ -Rho interaction. *STE4*^{A405V} cells show a significant decrease in the localization of activated Rho1 localization to the mating projection tip. Therefore, the G β γ of yeast recruits Rho1 to a particular membrane domain in response to an external signal. Given the known functions of Rho1, its association with G β γ could serve either of two purposes. Recruitment to the growth site during pheromone-induced projection formation would concentrate Rho1 in the place where stimulation of 1,3- β -glucan synthase activity is needed. Alternatively, G β γ might help position Rho1 in the vicinity of Pkc1, thereby facilitating Rho1 stimulation of the cell integrity MAP kinase cascade. In fact, pheromone induction of the Mpk1 MAP kinase requires Ste4 (50), and Rho1 is required to localize Pkc1 to sites of polarized growth (51). In either case, we would expect G β γ -Rho1 coupling to contribute to the chemotropic growth of the cell wall during mating. Consistent with this hypothesis, *STE4*^{A405V} compromises the integrity of pheromone-treated cells, which are partially deficient in Rho1 activity (Fig. 5). An intriguing possibility is that the recruitment of both Rho1 and Cdc42 to the pheromone-induced site of polarized growth by G β γ serves to coordinate cell wall and plasma membrane biosynthesis in time and space.

Acknowledgments—We thank Stephen Elledge for providing the lambda yeast cDNA library; Michael Hall, Yoshimi Takai, and Yoskikazu Ohya for providing *RHO1* strains and plasmids; Grace Park for technical assistance; and members of the Stone laboratory for critical reading of the manuscript.

REFERENCES

- Segall, J. E. (1993) *Proc. Natl. Acad. Sci. U. S. A.* **90**, 8332–8336
- Valtz, N., Peter, M., and Herskowitz, I. (1995) *J. Cell Biol.* **131**, 863–873
- Schrick, K., Garvik, B., and Hartwell, L. H. (1997) *Genetics* **147**, 19–32
- Metodieva, M. V., Matheos, D., Rose, M. D., and Stone, D. E. (2002) *Science* **296**, 1483–1486
- Butty, A. C., Pryciak, P. M., Huang, L. S., Herskowitz, I., and Peter, M. (1998) *Science* **282**, 1511–1516
- Nern, A., and Arkowitz, R. A. (1999) *J. Cell Biol.* **144**, 1187–1202
- Nern, A., and Arkowitz, R. A. (1998) *Nature* **391**, 195–198
- Adams, A. E., Johnson, D. I., Longnecker, R. M., Sloat, B. F., and Pringle, J. R. (1990) *Mol. Cell. Biol.* **11**, 131–142
- Klis, F. M. (1994) *Yeast* **10**, 851–869
- Drgonova, J., Drgon, T., Tanaka, K., Kollar, R., Chen, G.-C., Ford, R. A., Chan, C. S. M., Takai, Y., and Cabib, E. (1996) *Science* **272**, 277–279
- Levin, D. E., and Bartlett-Heubusch, E. (1992) *J. Cell Biol.* **116**, 1221–1229
- Lee, K. S., Irie, K., Gotoh, Y., Watanabe, Y., Araki, H., Nishida, E., Matsumoto, K., and Levin, D. E. (1993) *Mol. Cell. Biol.* **13**, 3067–3075
- Errede, B., and Levin, D. E. (1993) *Curr. Opin. Cell Biol.* **5**, 254–260
- Levin, D. E., Bowers, B., Chen, C. Y., Kamada, Y., and Watanabe, M. (1994) *Cell. Mol. Biol. Res.* **40**, 229–239
- Guthrie, C., and Fink, G. R. (eds) (1991) *Guide to Yeast Genetics and Molecular Biology*, Academic Press, San Diego, CA
- Ausubel, F. M., Brent, R., Kingston, R. E., Moore, D. D., Seidman, J. G., Smith, J. A., and Struhl, K. (1994) *Current Protocols in Molecular Biology* (Janssen, K., ed) John Wiley and Sons, Inc., New York
- Reed, S. I., Hadwiger, J. A., and Lorincz, A. T. (1985) *Proc. Natl. Acad. Sci. U. S. A.* **82**, 4055–4059
- Li, E., Meldrum, E., Stratton, H., and Stone, D. E. (1998) *Genetics* **148**, 947–961
- Ito, H., Fukuda, Y., Murata, K., and Kimura, A. (1983) *J. Bacteriol.* **153**, 163–168
- Madaule, P., Axel, R., and Myers, A. M. (1987) *Proc. Natl. Acad. Sci. U. S. A.* **84**, 779–783
- Trueheart, J., Boeke, J. D., and Fink, G. R. (1987) *Mol. Cell. Biol.* **7**, 2316–2328
- Slater, M. R., and Craig, E. A. (1987) *Mol. Cell. Biol.* **7**, 1906–1916
- Breeden, L., and Nasmyth, K. (1987) *Cell* **48**, 389–397
- Paravicini, G., Cooper, M., Friedli, L., Smith, D. J., Carpentier, J. L., Klig, L. S., and Payton, M. A. (1992) *Mol. Cell. Biol.* **12**, 4896–4905
- Cole, G. M., Stone, D. E., and Reed, S. I. (1990) *Mol. Cell. Biol.* **10**, 510–517
- Nomoto, S., Nakayama, N., Arai, K.-I., and Matsumoto, K. (1990) *EMBO J.* **9**, 691–696
- Whiteway, M., Hougan, I., and Thomas, D. Y. (1990) *Mol. Cell. Biol.* **10**,

- 217–222
28. Narumiya, S. (1996) *J. Biochem. (Tokyo)* **120**, 215–228
29. Kimura, K., Ito, M., Amano, M., Chihara, K., Fukata, Y., Nakafuku, M., Yamamori, B., Feng, J., Nakano, T., Okawa, K., Iwamatsu, A., and Kaibuchi, K. (1996) *Science* **273**, 245–248
30. Sahai, E., Olson, M. F., and Marshall, C. J. (2001) *EMBO J.* **20**, 755–766
31. Drgonova, J., Drgon, T., Roh, D.-H., and Cabib, E. (1999) *J. Cell Biol.* **146**, 373–387
32. Qadota, H., Python, C. P., Inoue, S. B., Arisawa, M., Anraku, Y., Zheng, Y., Watanabe, T., Levin, D. E., and Ohya, Y. (1996) *Science* **272**, 279–281
33. Kamada, Y., Qadota, H., Python, C. P., Anraku, Y., Ohya, Y., and Levin, D. E. (1996) *J. Biol. Chem.* **271**, 9193–9196
34. Levin, D. E., Fields, F. O., Kunisawa, R., Bishop, J. M., and Thorner, J. (1990) *Cell* **62**, 213–224
35. Stevenson, B. J., Rhodes, N., Errede, B., and Sprague, G. F. (1992) *Genes Dev.* **6**, 1293–1304
36. Masuda, T., Tanaka, K., Nonaka, H., Yamochi, W., Maeda, A., and Takai, Y. (1994) *J. Biol. Chem.* **269**, 19713–19718
37. Kim, J., Bortz, E., Zhong, H., Leeuw, T., Leberer, E., Vershon, A. K., and Hirsch, J. P. (2000) *Mol. Cell. Biol.* **20**, 8826–8835
38. Ayscough, K. R., and Drubin, D. G. (1998) *Curr. Biol.* **8**, 927–930
39. Yamochi, W., Tanaka, K., Nonaka, H., Maeda, A., Musha, T., and Takai, Y. (1994) *J. Cell Biol.* **125**, 1077–1093
40. Nonaka, H., Tanaka, K., Hirano, H., Fujiwara, T., Kohno, H., Umikawa, M., Mino, A., and Takai, Y. (1995) *EMBO J.* **14**, 5931–5938
41. Kraynov, V. S., Chamberlain, C., Bokoch, G. M., Schwartz, M. A., Slabaugh, S., and Hahn, K. M. (2000) *Science* **290**, 333–337
42. Sekiya-Kawasaki, M., Abe, M., Saka, A., Watanabe, D., Kono, K., Minemura-Asakawa, M., Ishihara, S., Watanabe, T., and Ohya, Y. (2002) *Genetics* **162**, 663–676
43. Saka, A., Abe, M., Okano, H., Minemura, M., Qadota, H., Utsugi, T., Mino, A., Tanaka, K., Takai, Y., and Ohya, Y. (2001) *J. Biol. Chem.* **276**, 46165–46171
44. Tanaka, E., and Sabry, J. (1995) *Cell* **83**, 171–176
45. Haugh, J., Jason, M., Codazzi, F., Teruel, M., and Meyer, T. (2000) *J. Cell Biol.* **151**, 1269–1279
46. Ducheck, P., and Rorth, P. (2001) *Science* **291**, 131–133
47. Harhammer, R., Gohla, A., and Shultz, G. (1996) *FEBS Lett.* **399**, 211–214
48. Alberts, A. S., Bouquin, N., Johnston, L. H., and Triesman, R. (1998) *J. Biol. Chem.* **273**, 8616–8622
49. Thodeti, C. K., Massoumi, R., Bindeslev, L., and Sjolander, A. (2002) *Biochem. J.* **365**, 157–163
50. Buehrer, B. M., and Errede, B. (1997) *Mol. Cell. Biol.* **17**, 6517–6525
51. Andrews, P. D., and Stark, M. J. (2000) *J. Cell Sci.* **113**, 2685–2693